

Vinculin Facilitates Cell Invasion into Three-dimensional Collagen Matrices*[§]

Received for publication, November 20, 2009, and in revised form, February 8, 2010. Published, JBC Papers in Press, February 24, 2010, DOI 10.1074/jbc.M109.087171

Claudia T. Mierke^{†1}, Philip Kollmannsberger[‡], Daniel Paranhos Zitterbart[‡], Gerold Diez[‡], Thorsten M. Koch[‡], Susanna Marg[§], Wolfgang H. Ziegler[§], Wolfgang H. Goldmann[‡], and Ben Fabry[‡]

From the [‡]Center for Medical Physics and Technology, Biophysics Group, Friedrich-Alexander-University of Erlangen-Nuremberg, 91052 Erlangen, Germany and [§]Interdisziplinäres Zentrum für Klinische Forschung Leipzig, Faculty of Medicine, University of Leipzig, 404103 Leipzig, Germany

The cytoskeletal protein vinculin contributes to the mechanical link of the contractile actomyosin cytoskeleton to the extracellular matrix (ECM) through integrin receptors. In addition, vinculin modulates the dynamics of cell adhesions and is associated with decreased cell motility on two-dimensional ECM substrates. The effect of vinculin on cell invasion through dense three-dimensional ECM gels is unknown. Here, we report how vinculin expression affects cell invasion into three-dimensional collagen matrices. Cell motility was investigated in vinculin knockout and vinculin expressing wild-type mouse embryonic fibroblasts. Vinculin knockout cells were 2-fold more motile on two-dimensional collagen-coated substrates compared with wild-type cells, but 3-fold less invasive in 2.4 mg/ml three-dimensional collagen matrices. Vinculin knockout cells were softer and remodeled their cytoskeleton more dynamically, which is consistent with their enhanced two-dimensional motility but does not explain their reduced three-dimensional invasiveness. Importantly, vinculin-expressing cells adhered more strongly to collagen and generated 3-fold higher traction forces compared with vinculin knockout cells. Moreover, vinculin-expressing cells were able to migrate into dense (5.8 mg/ml) three-dimensional collagen matrices that were impenetrable for vinculin knockout cells. These findings suggest that vinculin facilitates three-dimensional matrix invasion through up-regulation or enhanced transmission of traction forces that are needed to overcome the steric hindrance of ECMs.

Cell migration is an important and fundamental biomechanical process that plays an essential role in inflammatory diseases, embryonic development, wound healing, and metastasis formation. Current concepts of cell migration have been established in two-dimensional models, but they can explain only partially the migratory behavior in three dimensions. For

instance, the migratory capability of cells on two-dimensional substrates depends mainly on adhesion strength, adhesion dynamics, and the dynamics of cytoskeletal remodeling (1, 2), whereas the migratory capability of cells in three-dimensional connective tissue depends also on the steric hindrance of the matrix, matrix degradation by proteolytic enzyme secretion, and the generation of protrusive or contractile forces (1, 3–5). The balance of all these parameters—adhesion strength, cytoskeletal remodeling, matrix degradation, and the generation and transmission of contractile forces—is important for the migration speed in three-dimensional extracellular matrix (ECM)² (6). Depending on this balance, a broad variety of invasion strategies between different cell types and even within the same cell type are possible (7).

The connection between the ECM and the actomyosin cytoskeleton through integrin-type cell-matrix adhesion receptors is facilitated by the mechano-coupling protein vinculin (8, 9). The effect of vinculin on the migration of cells has previously been investigated using two-dimensional ECM substrates, where decreased vinculin expression caused increased cell migration (10). This finding has been explained by increased paxillin and focal adhesion kinase phosphorylation (11) and increased turnover of focal adhesions (12). In a recent study, we reported that vinculin acts as a mechano-regulating protein by increasing the generation of contractile forces (9). Because increased contractile forces are thought to facilitate three-dimensional cell invasion, we hypothesize that vinculin-expressing cells show higher invasiveness into three-dimensional ECMs. Hence, we suggest here that the inhibitory effect of vinculin on two-dimensional ECM migration is not present during three-dimensional ECM invasion.

The aim of this study is to test this prediction. We analyzed the migratory behavior of mouse embryonic fibroblasts wild-type (MEFvin^{wt/wt}) and vinculin-deficient (MEFvin^{-/-}) cells on two-dimensional ECM substrates and in three-dimensional ECM. We found that MEFvin^{wt/wt} cells were 3-fold more invasive compared with MEFvin^{-/-} cells. RNA interference-mediated vinculin knockdown in MEFvin^{wt/wt} cells considerably reduced their invasiveness into three-dimensional ECMs.

* This work was supported, in whole or in part, by National Institutes of Health Grant HL65960. This work was also supported by Deutsche Forschungsgemeinschaft Grants FA336/2-1 and GO598/13-1, the Cluster of Excellence "Engineering of Advanced Materials" Program, Deutsche Krebshilfe Grant 107384, Deutscher Akademischer Austausch Dienst, Bavaria California Technology Center, and Bayerisch-Französisches Hochschulzentrum.

[§] The on-line version of this article (available at <http://www.jbc.org>) contains supplemental Figs. S1 and S2.

[†] To whom correspondence should be addressed: University of Erlangen-Nuremberg, Center for Medical Physics and Technology, Biophysics Group, Henkestr. 91, 91052 Erlangen, Germany. Tel.: 49-9131-85-25607; Fax: 49-9131-85-25601; E-mail: claudia.mierke@t-online.de.

² The abbreviations used are: ECM, extracellular matrix; MEF, mouse embryonic fibroblast; DMEM, Dulbecco's modified Eagle's medium; PBS, phosphate-buffered saline; FACS, fluorescence-activated cell sorter; MMP, matrix metalloproteinase; MT1, membrane type 1; FN, fibronectin; MSD, mean square displacement; siRNA, small interfering RNA; vin-siRNA, vinculin-specific siRNA.

Vinculin Facilitates Cell Invasion

Using Fourier transform traction microscopy, we found that MEFvin^{wt/wt} cells generated 3-fold higher contractile forces compared with MEFvin^{-/-} cells, suggesting that vinculin-mediated enhanced contractility contributed to the ability of invading cells to overcome the steric hindrance of three-dimensional ECMs.

EXPERIMENTAL PROCEDURES

Cell Lines and Cell Culture—Mouse embryonic wild-type fibroblasts (MEFvin^{wt/wt}) as well as vinculin-deficient fibroblasts (MEFvin^{-/-}) were derived from littermate embryos (embryonic day 9) of mice carrying a vinculin null allele that lacks vinculin exon 3 (21). A reason for the new generation of MEFs was that MEFs from E. D. Adamson might be altered by several passages in different laboratories and by environmental influences. We therefore generated independent populations of MEFvin^{wt/wt} and MEFvin^{-/-} cells derived from a recent mating of the same mouse line. The latter populations were immortalized using largeT antigen transfection and were used as control for vinculin-independent effects of immortalization. Invasion experiments were performed with both sets of MEFvin^{wt/wt}/MEFvin^{-/-} populations, and no significant differences were observed for the experiments reported in this manuscript (data not shown). Newly MEFs were used in Figs. 1, 2, and 6, and Adamson MEFs were used for the experiments presented in Figs. 3–5.

The cells were maintained in low glucose (1 g/liter, Adamson cells; cells grow too rapidly in high glucose medium) or high glucose (4.5 g/liter, new MEF populations) Dulbecco's modified Eagle's medium supplemented with 10% fetal calf serum (low endotoxin), 2 mM L-glutamine, and 100 units/ml penicillin-streptomycin (DMEM complete medium; all from Biochrom, Berlin, Germany). The cells were harvested with Accutase after they had reached 80% confluency. The percentage of dead cells after detachment with Accutase was less than 1%. Mycoplasma contamination was excluded using a mycoplasma detection kit (Roche Applied Science). All of the chemicals were purchased from Sigma unless otherwise indicated.

Three-dimensional Collagen Invasion Assay—For the preparation of 5.8 mg/ml collagen matrices, 0.775 ml of collagen R (2 mg/ml rat collagen type I; Serva, Heidelberg, Germany), 1.95 ml of collagen R (10.68 mg/ml rat collagen type I; Becton Dickinson, Heidelberg, Germany), and 0.775 ml of collagen G (4 mg/ml bovine collagen type I; Biochrom) were mixed. After the addition of 0.4 ml of NaHCO₃ buffer (26.5 mM) and 0.4 ml of 10× DMEM, the mixture was neutralized, pipetted into 3.5-cm dishes, and polymerized at 37 °C, 5% CO₂, and 95% humidity for 2 h. Then 2 ml of DMEM complete medium was pipetted on top of the gels and incubated at 37 °C, 5% CO₂, and 95% humidity overnight (13). Other matrices with lower collagen concentrations (2.4 and 3.7 mg/ml) were obtained by dilution of the non-polymerized 5.8 mg/ml collagen mixture with PBS buffer. 100,000 cells were seeded on top of the collagen matrix and cultured for 72 h. At this time period, the differences in the invasiveness of cells were clearly visible. After fixation with 2.5% glutaraldehyde solution in PBS, the number of invaded cells and their invasion depth were determined in 12 randomly selected fields of view. To determine the percentage of invaded

cells, the adherent cells on top of the collagen fiber network were also counted.

Vinculin Knockdown—200,000 MEFvin^{wt/wt} cells were seeded in Ø 3.5-cm dishes and cultured in 2 ml of DMEM complete medium. 5 µl of a 20 µM vinculin RNA interference solution (target sequence CAGAATTATGTGATGATCCTA), 12 µl of HiPerFect reagent (Qiagen), and 100 µl of DMEM were mixed. Before addition to the cells, we let the mixture rest for 10 min at room temperature. RNA interference-mediated vinculin-knockdown was confirmed after 1, 2, and 3 days using Western blotting. Transfection efficiency was 99% as confirmed by FACS analysis using 20 µM Alexafluor546-labeled control siRNA (Allstar; Qiagen).

Inhibition of Enzymatic Degradation—To inhibit enzymatic degradation of the ECM, we added 100 µM of the broad spectrum matrix metalloproteinase (MMP) inhibitor GM6001 (14). To test whether the GM6001 inhibitor is functional in our invasion assay, we used invasive MDA-MB-231 breast cancer cells and could show that their invasiveness decreased after inhibitor addition (data not shown).

Flow Cytometry—For flow cytometry measurements of integrin and membrane type 1 (MT1)-MMP cell surface expression levels, the cells were harvested, resuspended in HEPES buffer (20 mM HEPES, 125 mM NaCl, 45 mM glucose, 5 mM KCl, 0.1% albumin, pH 7.4), and incubated with primary rat antibodies directed against mouse αv integrin subunit (CD51, rat IgG1, clone RMV-7; Chemicon, Temecula, CA), β1 integrin subunit (CD29, rat IgG2, clone MB1.2; Chemicon), and α5β1 integrin (VLA-5, rat IgG, clone BMA5; Chemicon). For MT1-MMP detection, we used a mouse monoclonal anti-human/mouse MT1-MMP antibody (mouse IgG1; R & D Systems). Isotype-matched IgG antibodies were used as control (all from Caltag, Burlingame, CA). After 30 min of incubation at 4 °C, the cells were washed and stained with a secondary antibody (R-phycoerythrin-labeled donkey anti-rat IgG (F(ab)₂ fragment) or R-phycoerythrin-labeled goat anti-mouse IgG (F(ab)₂ fragment); both from Dianova). Analysis by flow cytometry was performed using a FACSCalibur system (Becton Dickinson).

Cell Spreading and Immunofluorescence—100,000 cells were seeded on glass coverslips (Menzel, Braunschweig, Germany) that were coated with 50 µg/ml collagen type I for 1 h at 37 °C. After 4 and 24 h, adherent cells were fixed using 3% paraformaldehyde solution for 15 min at room temperature. The cells were washed with PBS buffer twice and stained for 30 min at room temperature with 66 nM Alexafluor546 Phalloidin (Molecular Probes, Eugene, Oregon) in 3% paraformaldehyde solution containing 500 µg/ml L-α-lysophosphatidylcholine. Finally, the cell nuclei were stained using 1 mg/ml Hoechst dye 33342 for 5 min at room temperature. The cells were embedded in 30 µl of Vectashield mounting medium (Vector Laboratories, Burlingame, CA). 10–20 fields of view (20× magnification) were recorded randomly for each cell line. The cells were counted in each image, and the projected area (spreading area) was computed using a custom image processing program written in MATLAB.

Immunofluorescence—After paraformaldehyde fixation, the cells were permeabilized with PBS containing 0.1% Triton X-100 for 5 min at room temperature. After washing, the cells

were blocked with DMEM complete medium and stained for 30 min at room temperature with a primary antibody directed against vinculin (Sigma) or paxillin (Chemicon), each diluted 1:200 in DMEM. After washing, the cells were incubated with a secondary Cy2-labeled antibody directed against mouse IgG (1:200) and with 66 nM Alexa Fluor 546 Phalloidin in DMEM complete medium. The cell nuclei were stained with 1 mg/ml Hoechst dye 33342 for 5 min, and finally the cells were embedded in 30 μ l of Mowiol solution (Sigma). 10–20 randomly selected fields of view were recorded at 40 \times magnification.

Magnetic Tweezer—For creep measurements, a staircase-like sequence of step forces ranging from 0.5 to 10 nN was applied to superparamagnetic 4.5- μ m epoxytated and fibronectin (FN)-coated beads (100 μ g/ml FN in PBS at 4 $^{\circ}$ C for 24 h; Roche Applied Science) using a magnetic tweezer (9, 13, 15). After FN coating, the beads were washed in PBS and stored at 4 $^{\circ}$ C. Prior to measurements, the beads were sonicated, added to the cells (2×10^5 beads/ 1×10^5 cells), and incubated at 5% CO₂ and 37 $^{\circ}$ C. After 30 min of bead incubation, measurements were performed at 37 $^{\circ}$ C on an inverted microscope (DMI Leica) with 40 \times magnification. When a force step with an amplitude ΔF was applied to a cell-bound bead, it moved with a displacement $d(t)$ toward the tip of the tweezer needle. The ratio $d(t)/\Delta F$ defines a creep response $J(t)$. $J(t)$ of the cells followed a power law with time, $J(t) = a(t/t_0)^b$, where the prefactor, a , and the power law exponent, b , were both force-dependent, and the reference time, t_0 , was set to 1 s. The coefficients a and b were determined by a least squares fit (9). The prefactor a (units of μ m/nN) characterizes the elastic cell properties and corresponds to a compliance (*i.e.* inverse of stiffness) (9). b reflects the dynamics of the force-bearing structures of the cell that are connected to the bead (16). A power law exponent of $b = 0$ is indicative of a purely elastic solid, and $b = 1$ is indicative of a purely viscous fluid (16). In cells, the power law exponent usually falls in the range between 0.1 and 0.5, whereby higher values have been linked to a higher turnover rate of cytoskeletal structures. Moreover, higher b values are often associated with reduced cell stiffness (16).

Bead Detachment—50,000 cells were seeded into \emptyset 3.5-cm dishes. After 2 days, the cells were incubated with FN-coated beads for 30 min at 37 $^{\circ}$ C, 5% CO₂, and 95% humidity. The detachment of FN-coated beads from the cells was measured during force application ranging from 0.5 to 10 nN. The percentage of detached beads in relation to the detachment force was used to quantify the bead binding strength to the cell. To test whether the FN-coated beads bind specifically to integrin receptors, we added 10 μ g/ml of the adhesion blocking anti-CD29 (β 1 integrin, clone 9EG7; BD) monoclonal antibody to the cells 30 min prior to FN bead addition.

Traction Microscopy—Gels for traction experiments were cast on rectangular 75 \times 25-mm nonelectrostatic silane-coated glass slides (17). Gels with 6.1% acrylamide, 0.24% bis-acrylamide were used. The Young's modulus of the gels was 13 kPa. Yellow-green fluorescent 0.5- μ m carboxylated beads (Invitrogen) were suspended in the gels and centrifuged at 300 \times g toward the gel surface during polymerization at 4 $^{\circ}$ C (18). These beads served as markers for gel deformation. The surface of the gel was activated with Sulfo-SANPAH (Pierce) and coated with

50 μ g/ml collagen type I. The cell suspension added to the gel was contained in a silicone ring (flexi-perm; In Vitro, Göttingen, Germany) attached to a glass slide. We seeded MEFvin^{wt/wt} and MEFvin^{-/-} cells on top of collagen-coated polyacrylamide gels and cultured them overnight to let them completely adhere. Cell tractions were computed from an unconstrained deconvolution of the gel surface displacement field measured before and after cell detachment using a drug mixture of cytochalasin D (15 μ M), ML-7 (15 μ M), and trypsin/EDTA (10 \times) (19). Gel deformations were estimated using a Fourier-based difference-with-interpolation image analysis (18). The strain energy was calculated as the product of local tractions and matrix deformations, integrated over the spreading area of the cell (19).

Migration Assay—50,000 cells were seeded into 3.5-cm dishes coated with 50 μ g/ml collagen type I. After 30 min, the cells were placed in a microscope incubation chamber (37 $^{\circ}$ C, 5% CO₂), and phase contrast images were recorded every minute for 2 h (10 \times magnification). The cell movements were computed using a Fourier-based difference-with-interpolation image analysis (18). These cells moved spontaneously with a mean square displacement (MSD) that also followed a power law with time, $MSD = D \cdot (t/t_0)^\beta$, where t_0 is the time interval of the image recordings (1 min), the prefactor D is the apparent diffusivity, equivalent to the square of the distance traveled during 1-min intervals, and the power law exponent β is a measure of the persistence, with $\beta = \sim 1$ for randomly migrating cells and $\beta = \sim 2$ for directed, ballistic motion along a straight path (18).

Statistics—The data are expressed as the mean values \pm S.E., if not indicated otherwise. Statistical analysis was performed using a two-tailed paired t test. $p < 0.05$ was considered to be statistically significant.

RESULTS

Function of Vinculin in Cell Motility—Here, we analyze the effect of vinculin on cell invasion using MEFvin^{-/-} and MEFvin^{wt/wt}. Cell invasion into dense three-dimensional collagen matrices was analyzed after 3 days of culture. Invasive MEFvin^{wt/wt} and MEFvin^{-/-} cells were spindle-shaped (Fig. 1A). MEFvin^{wt/wt} control cells showed a higher percentage of invasive cells compared with vinculin-deficient MEFs ($32.9 \pm 3.5\%$ versus $0.5 \pm 0.1\%$; Fig. 1B). The invasion profiles expressed as the cumulative probability of finding a cell at or below a given invasion depth reveal that MEFvin^{wt/wt} cells invade much deeper into three-dimensional collagen matrices compared with MEFvin^{-/-} cells (Fig. 1C). To confirm that the differences between MEFvin^{wt/wt} and MEFvin^{-/-} cell lines were caused by different levels of vinculin expression and not by other confounding effects, we analyzed MEFvin^{wt/wt} cells that were treated for 24 h prior to the start of the invasion assay with vinculin-specific siRNA (vin-siRNA) or nonspecific control siRNA. Immunoblot analysis in vin-siRNA-treated cells revealed that vinculin protein expression was reduced to less than 50% of wild-type levels after 1 day and was not detectable after 2–3 days of treatment (supplemental Fig. S2). After 3 days of culture on collagen matrices, the fraction of invasive cells and the invasion profile were determined. Invasive control siRNA

Vinculin Facilitates Cell Invasion

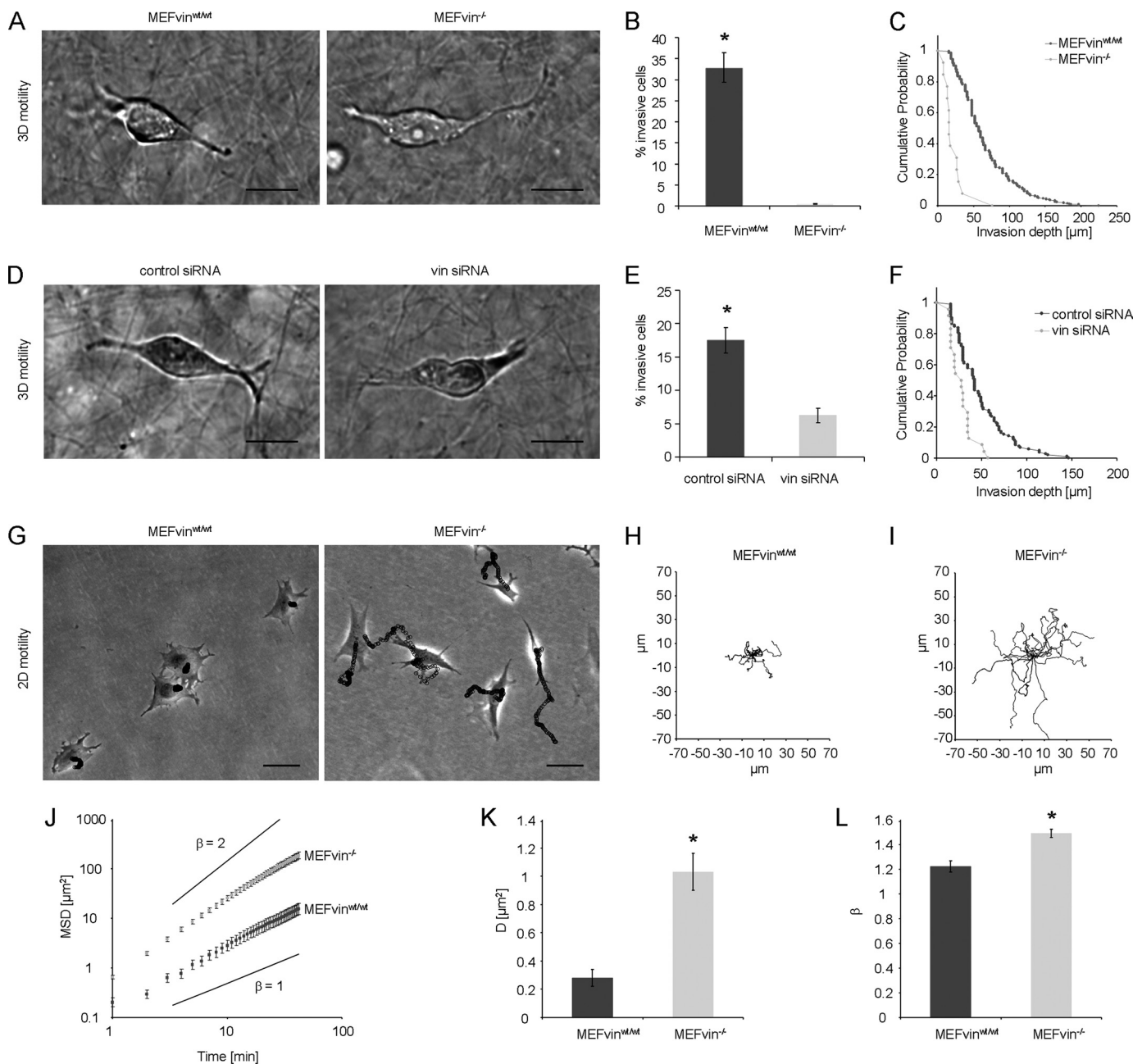


FIGURE 1. Vinculin dependence of cell invasion into collagen gels (three-dimensional, 3D) compared with cell migration on collagen substrates (two-dimensional, 2D). *A*, modulation contrast images of a representative invasive MEFvin^{wt/wt} cell (*left panel*) and a MEFvin^{-/-} cell (*right panel*) after 3 days of invasion into collagen gels (invasion depth, 50 μm). *Scale bars*, 20 μm . *B*, the percentage of invasive MEFvin^{wt/wt} cells is higher compared with MEFvin^{-/-} cells. *C*, the cumulative probability shows increased depth of invasion for MEFvin^{wt/wt} cells. *D*, modulation contrast images of representative invasive MEFvin^{wt/wt} cells after 3 days of invasion into collagen gels treated with control siRNA (*left panel*) or vin-siRNA (*right panel*). *Scale bars*, 20 μm . *E*, the percentage of invasive cells is 2.5-fold higher in control siRNA as compared with vin-siRNA treated cells. *F*, the invasion profile shows that control siRNA treated cells invade deeper into collagen gels than vin-siRNA-treated cells. *G*, phase contrast images and trajectories of MEFvin^{wt/wt} (*left panel*) and MEFvin^{-/-} cells (*right panel*) on collagen-coated glass. *Scale bars*, 30 μm . *H* and *I*, the motion of MEFvin^{wt/wt} (*H*) and MEFvin^{-/-} cells (*I*) was recorded over 2 h, and the starting points of the trajectories lines were transposed to the same origin. *J*, MSD calculated from trajectories of MEFvin^{-/-} cells (*light gray*) was significantly larger than that of MEFvin^{wt/wt} cells (*dark gray*). *K* and *L*, the apparent diffusivity *D* (*K*) and the persistence β (*L*) of cell motility were significantly increased in MEFvin^{-/-} compared with MEFvin^{wt/wt} cells ($n > 55$ cells; $p < 0.05$).

and vin-siRNA treated MEFvin^{wt/wt} cells were equally spindle-shaped as invasive MEFvin^{wt/wt} and MEFvin^{-/-} cells (Fig. 1*D*). Control siRNA cells showed a 3-fold higher number of invasive cells compared with vin-siRNA-treated cells (Fig. 1*E*). Furthermore, the invasion profiles showed that control siRNA cells were capable of invading much more deeply into three-dimensional collagen matrices compared with vin-siRNA-treated cells (Fig. 1, *D–F*). These data confirm that the differences in cell

invasion between MEFvin^{wt/wt} and MEFvin^{-/-} cells were caused by vinculin and not by some other differences.

The strongly reduced three-dimensional collagen invasiveness of MEFvin^{-/-} cells was surprising, because these cells have been previously reported to exhibit increased motility and migration speed on two-dimensional surfaces (20, 21). To investigate this, we analyzed the two-dimensional motility of both cell lines also on collagen type I-coated glass coverslips

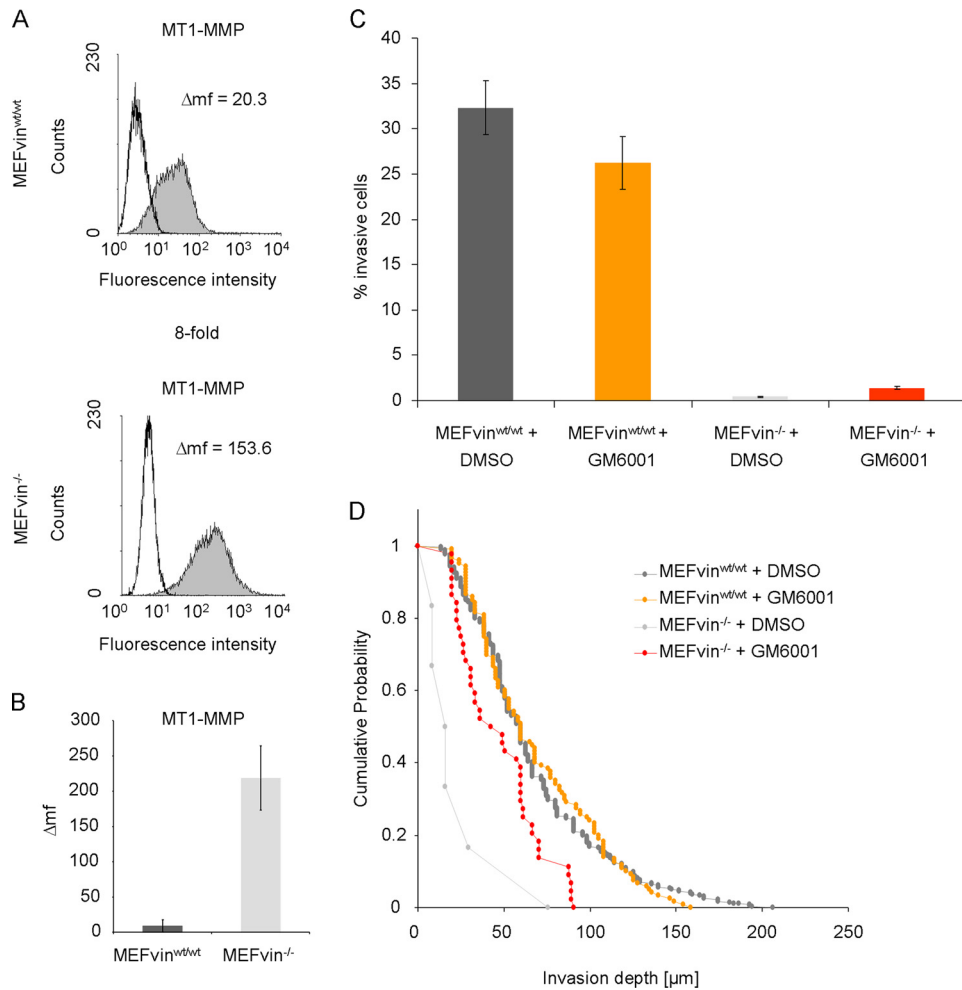


FIGURE 2. Effect of MMP-inhibition and MT1-MMP expression on cell invasion. *A*, FACS analysis of MT1-MMP expression in MEFvin^{wt/wt} and MEFvin^{-/-} cells. The numbers in the histograms specify the differences in the mean fluorescence intensities (Δmf) between specific antibody binding (shaded gray curves) and appropriate isotype controls (white curves). MT1-MMP receptor expression was increased in MEFvin^{-/-} cells (*A* and *B*). *B*, mean values (Δmf) \pm S.E. of three to five independent FACS measurements. *C*, the percentages (means \pm S.E.) of invasive cells treated with 100 μM GM6001 was slightly decreased in MEFvin^{wt/wt} and slightly increased in MEFvin^{-/-} compared with dimethyl sulfoxide (DMSO) control treatment. *D*, the invasion profile of MEFvin^{wt/wt} cells treated with GM6001 (orange) was unchanged compared with dimethyl sulfoxide control treatment (dark gray), whereas the invasion profile of MEFvin^{-/-} cells treated with GM6001 (light gray) revealed more invasive behavior compared with the dimethyl sulfoxide control (red).

and confirmed that MEFvin^{-/-} cells show an ~ 3 -fold higher migration speed in two-dimensional than MEFvin^{wt/wt} cells (Fig. 1, *G–L*). The speed and persistence of cell migration was further investigated by analyzing the time evolution of the MSD of the cells (Fig. 1*J*). The MSD increased with time according to a power law relationship (22): $MSD = D(t/t_0)^\beta$, where t_0 is the time interval, the prefactor D is the apparent diffusivity, and the exponent β is a measure of the persistence. The apparent diffusivity D was 4-fold increased in MEFvin^{-/-} cells compared with MEFvin^{wt/wt} cells (Fig. 1*K*). In addition, MEFvin^{-/-} cells migrated more persistently ($\beta = 1.5$) compared with MEFvin^{wt/wt} cells ($\beta = 1.2$) (Fig. 1, *J* and *L*). Together, these results establish that vinculin has different effects on two-dimensional versus three-dimensional cell motility: MEFvin^{-/-} cells show increased motility on two-dimensional substrates but decreased invasion in three-dimensional collagen matrices. In the following, we

studied the possible mechanisms that may account for these different effects.

Role of Matrix Degradation for Vinculin-mediated Cell Invasiveness—Cell migration has been reported to be augmented by the secretion of the MT1-MMP that degrades the surrounding ECM (7). Here, we tested whether differences in MT1-MMP cell surface expression were responsible for differences in cell invasiveness between MEFvin^{wt/wt} and MEFvin^{-/-} cells. Analysis by flow cytometry revealed an 8-fold up-regulation of MT1-MMP in MEFvin^{-/-} cells (Fig. 2, *A* and *B*), yet this up-regulation was insufficient to cause significant degradation of the matrix to a level that would have promoted MEFvin^{-/-} cell invasion into three-dimensional ECMs. Rather, this large MT1-MMP secretion may have attenuated invasiveness by interfering with integrin-ECM binding (23). To investigate this possibility, we added the matrix-metalloproteinase inhibitor GM6001 (100 μM) prior to the start of the invasion assay. In MEFvin^{wt/wt} cells, we found that the invasion profile was unchanged, and the percentage of invasive cells was slightly reduced after GM6001 treatment (Fig. 2*C*). In MEFvin^{-/-} cells, both the percentage of invasive cells and the average invasion depths were slightly increased after GM6001 treatment (Fig. 2*D*). Taken together, however, these data show that matrix-metalloproteases do

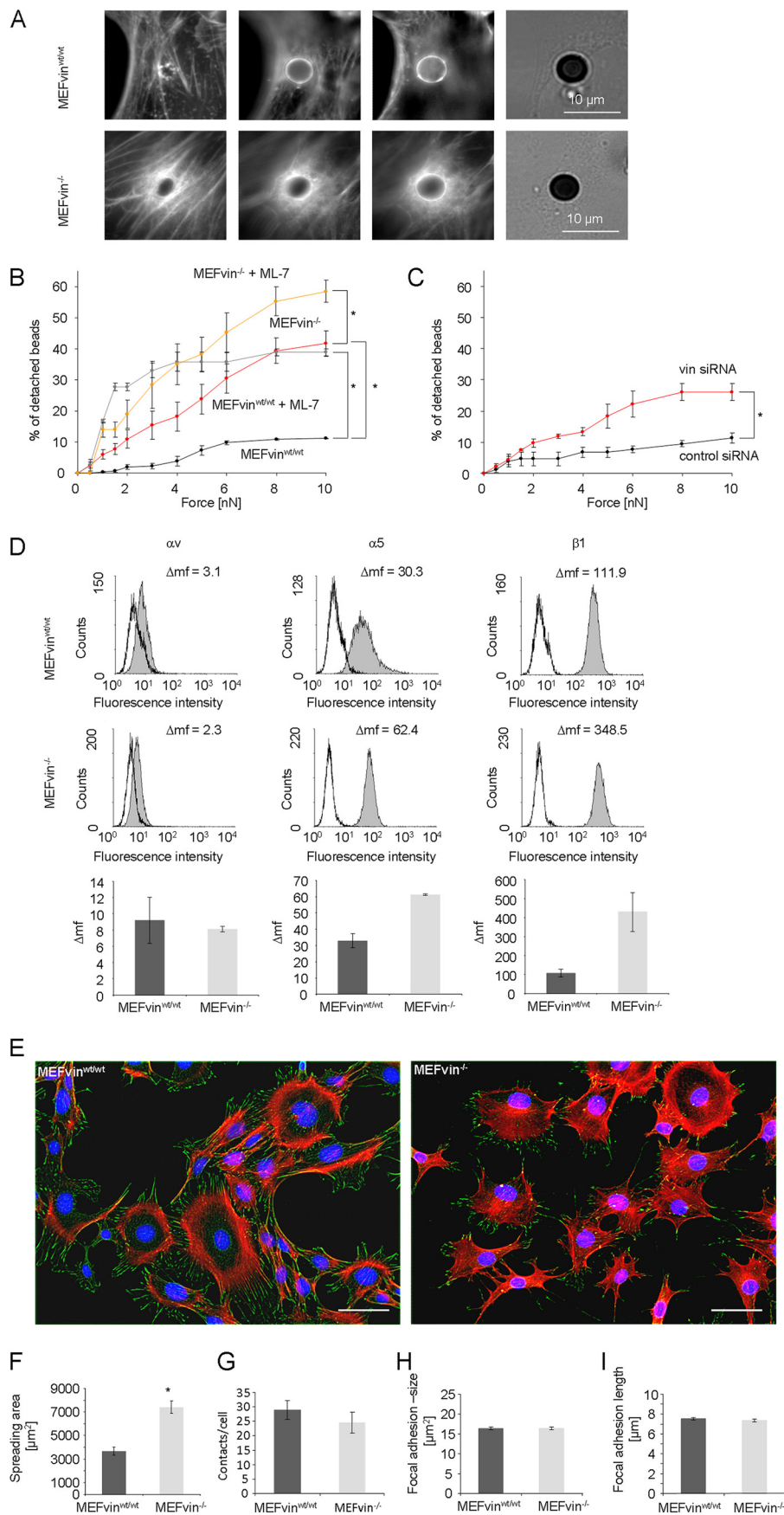
not play a significant role in vinculin-facilitated cell invasion.

Vinculin Increases Adhesion Strength—To analyze whether differences in cell motility between MEFvin^{wt/wt} and MEFvin^{-/-} cells are due to vinculin-facilitated differences in adhesion strength, we measured the mechanical stability of the focal adhesions by applying forces to FN-coated superparamagnetic beads attached to cell surface integrins. The binding of these beads to integrins induced local actin remodeling such as the accumulation of actin and the assembly of stress fibers around the bead both in MEFvin^{wt/wt} and MEFvin^{-/-} cells (Fig. 3*A*). FN is a ligand for the $\alpha 5 \beta 1$ integrin receptor that is highly expressed on these MEFs (Fig. 3*C*). The binding of FN-coated beads was inhibited by more than 90% after the addition of 10 $\mu g/ml$ $\beta 1$ integrin subunit (CD29) neutralizing antibody 10 min prior to bead addition to MEFvin^{wt/wt} cells (data not shown), demonstrating that FN-coated beads bind specially to $\alpha 5 \beta 1$ integrins.

Vinculin Facilitates Cell Invasion

To quantify the adhesion strength, stepwise increasing forces between 0.5 and 10 nN were applied to the beads using magnetic tweezers. The force value at which a bead detached from the cell surface was measured. For forces above 1 nN, the fraction of beads that detached from the cell surface was more than 2-fold higher in MEFvin^{-/-} cells compared with MEFvin^{wt/wt} cells (Fig. 3B). The low adhesion strength of MEFvin^{-/-} cells was caused neither by low bead internalization (supplemental Fig. S1) nor by low integrin expression (Fig. 3D). In fact, the expression of the FN receptor integrin subunits $\alpha 5$ and $\beta 1$ were even 2-fold up-regulated on MEFvin^{-/-} cells (Fig. 3C). Moreover, the expression of the collagen-binding integrin receptor subunits αv (Fig. 3C) and $\alpha 4$ (data not shown) was similar to that of MEFvin^{wt/wt} cells, and the collagen-binding integrin receptor $\alpha 2$ was not detectable on both MEFs (data not shown).

Effect of Vinculin on Focal Adhesions and Spreading Area—To test whether the differences in two-dimensional and three-dimensional motility and adhesion strength between MEFvin^{-/-} cells and MEFvin^{wt/wt} cells were correlated with vinculin-mediated alterations in focal adhesion morphology, we stained MEFvin^{wt/wt} and MEFvin^{-/-} cells using an anti-paxillin antibody. The cells were plated on collagen type I-coated glass coverslips using the same collagen that was used for three-dimensional ECMs. After a plating time of 24 h, the spreading area of MEFvin^{-/-} cells was markedly increased compared with MEFvin^{wt/wt} cells (Fig. 3, D and E). The size and the length of the focal adhesions were not different (Fig. 3, G and H), and the number of focal adhesion contacts/cell was slightly but not significantly reduced in MEFvin^{-/-} cells after 24 h (Fig. 3F). Similar results were obtained for uncoated glass surfaces and for plating times of 4 h (data not shown). Because of their larger spreading area, the number density of focal adhesions (number of



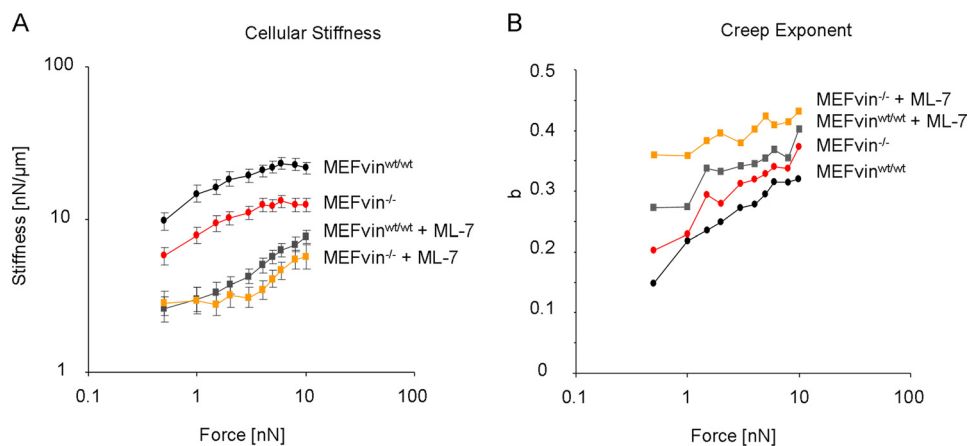


FIGURE 4. Effect of vinculin expression on stiffness and fluidity of cells. Cell stiffness (A; means \pm S.E.) and cell fluidity (B) of MEFvin^{wt/wt} (black) and MEFvin^{-/-} cells (red) was measured before (circles) and after (squares) inhibition of myosin light chain kinase with ML-7 and of MEFvin^{wt/wt} (dark gray) and MEFvin^{-/-} cells (orange).

focal adhesions/unit of spreading area) was markedly reduced in MEFvin^{-/-} cells (2-fold), which may have contributed to their weaker adhesion strength and hence their higher two-dimensional motility and impaired three-dimensional motility.

Vinculin Influences Cytoskeletal Dynamics and Cell Stiffness—To analyze whether a change in three-dimensional motility of vinculin-expressing cells was associated with altered cell stiffness and remodeling dynamics of the cytoskeleton, we performed microrheology measurements. Using magnetic tweezers, we applied forces of up to 10 nN to FN-coated superparamagnetic beads that were bound to integrin receptors (Fig. 3A). Bead displacement after a step increase in force, normalized to force magnitude, defines a creep response $J(t) = a \cdot (t/t_0)^b$ that can be subdivided into an elastic response (cell elasticity or stiffness, $1/a$) and a frictional response (cytoskeletal fluidity, b) (9, 24). MEFvin^{-/-} cells displayed higher cytoskeletal fluidity and lower stiffness compared with MEFvin^{wt/wt} cells, indicating that MEFvin^{-/-} cells are more deformable and therefore should be able to squeeze more easily through a dense matrix. Hence, the higher cytoskeletal fluidity and the decreased stiffness of MEFvin^{-/-} cells cannot explain their decreased invasiveness in three-dimensional ECMs.

In both cell lines, the cytoskeletal fluidity and stiffness increased with increasing forces (Fig. 4). This suggests that both MEFs respond to external forces through stress stiffening and increased fluidization of the actomyosin cytoskeleton independently of vinculin mechano-coupling function. The inhibition of contractile forces after the addition of the myosin light

chain kinase inhibitor ML-7 increased cellular fluidity in both cell lines (Fig. 4A). This indicates that the cell fluidity depends on the cell contractility. Interestingly, the cell stiffness of both cell lines decreased to nearly similar levels after the addition of the myosin light chain kinase inhibitor ML-7, indicating that the higher initial stiffness of the MEFvin^{wt/wt} cells prior to ML-7 addition may have been due to higher actomyosin-mediated contractile forces (Fig. 4B).

Vinculin Increases Contractile Force Generation—The contractile forces of spread cells are predominantly transmitted to the ECM as

opposed to internal compression-bearing elements such as microtubules (25). We measured contractile forces using two-dimensional traction microscopy and characterized the contractility of each cell by the elastic strain energy stored in the ECM because of the cell tractions. The strain energy of MEFvin^{wt/wt} cells was 3-fold higher (0.44 ± 0.05 pJ) compared with MEFvin^{-/-} cells (0.15 ± 0.06 pJ) (Fig. 5). This finding supports the hypothesis that the higher invasiveness of MEFvin^{wt/wt} cells was facilitated by higher contractile forces and higher tractions that helped them to overcome the steric hindrance of the ECM.

Effect of the Steric Hindrance on Vinculin-facilitated Cell Invasion—To test the hypothesis that the steric hindrance of the ECM accounts for low three-dimensional invasiveness in MEFvin^{-/-} cells, we further increased the steric hindrance by increasing the collagen concentration to 3.7 and 5.8 mg/ml. In agreement with our expectations, MEFvin^{wt/wt} cells were still able to invade collagen gels with higher concentrations (3.7 and 5.8 mg/ml; Fig. 6A, dark gray bar), whereas MEFvin^{-/-} cells were not (Fig. 6A, light gray bar).

DISCUSSION

In previous studies, we and others showed that decreased expression of the focal adhesion protein vinculin increased cell motility on a two-dimensional collagen-coated substrate (10, 20). In contrast to a two-dimensional collagen-coated substrate, here we report that cell invasion in a three-dimensional collagen matrix is decreased by knockout or knockdown of vinculin, suggesting that the effect of vinculin on cell motility

FIGURE 3. Effect of vinculin expression on adhesion strength, integrin expression, focal adhesions, and spreading area. A, fluorescent images recorded at different focus depths show that FN-coated beads are tightly associated with actin stress fibers (stained with Alexafluor546 Phalloidin) in MEFvin^{wt/wt} (top row) and MEFvin^{-/-} cells (bottom row). B, percentage of beads detached from the cells versus pulling force. Adhesion strength was significantly lower in MEFvin^{-/-} cells (red circles) compared with MEFvin^{wt/wt} cells (black circles). Addition of the MLCK inhibitor ML-7 decreased adhesion strength of MEFvin^{wt/wt} (light gray) and MEFvin^{-/-} cells (orange). *, $p < 0.05$. C, adhesion strength was significantly lower in vin-siRNA cells (red) compared with control siRNA cells (black). *, $p < 0.05$. D, FACS analysis of α v, α 5, and β 1 integrin subunit expression on MEFvin^{wt/wt} cells and MEFvin^{-/-} cells. The numbers in the histograms specify the differences in mean the fluorescence intensities (Δmf) between specific antibody binding (shaded gray curves) and appropriate isotype controls (white curves). α 5 as well as β 1 integrin subunit expression was increased in MEFvin^{-/-} cells, whereas the α v expression was not altered. The bar graphs show the mean values (Δmf) \pm S.E. of three to five independent FACS measurements. E, MEFvin^{wt/wt} and vin^{-/-} cells adhered for 24 h on collagen type I-coated glass. Actin was stained with Alexafluor546 Phalloidin (red), focal adhesions with an antibody directed against paxillin (green), and nuclei with Hoechst 33342 (blue). Scale bars are 30 μ m. F, spreading area (means \pm S.E.) of MEFvin^{-/-} cells (light gray) was significantly increased compared with MEFvin^{wt/wt} cells (dark gray). *, $p < 0.05$. G, numbers of focal adhesions/cell were slightly reduced in MEFvin^{-/-} cells. H and I, focal adhesion size (H) and focal adhesion length (I) showed no differences.

Vinculin Facilitates Cell Invasion

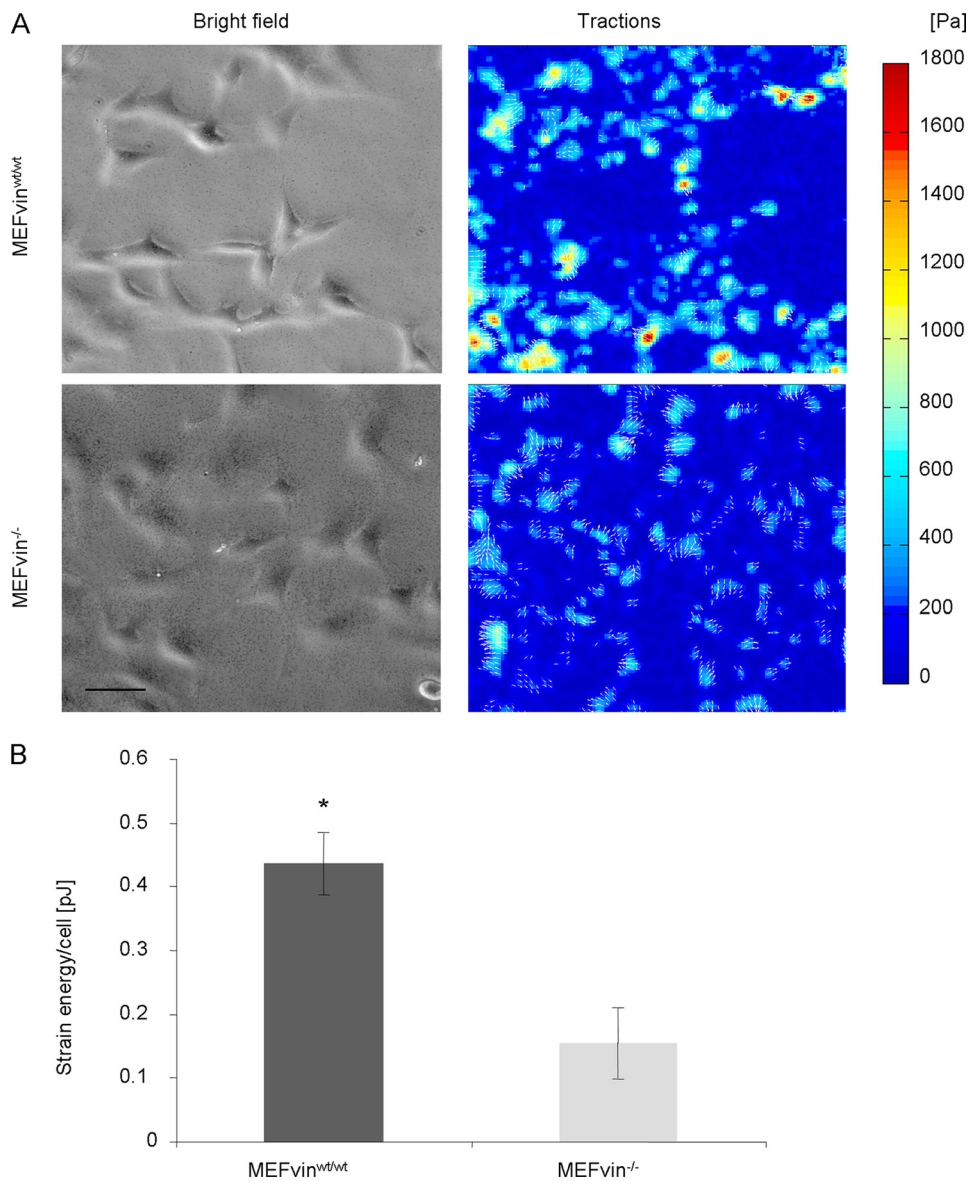


FIGURE 5. Effect of vinculin on the generation of contractile forces. *A*, bright field (*left panels*) and traction images (*right panels*) of MEFvin^{wt/wt} (*top panels*) and MEFvin^{-/-} cells (*bottom panels*). *B*, the strain energy/cell (means \pm S.E.) of MEFwt cells ($n = 191$) was 3-fold increased compared with MEFvin^{-/-} cells ($n = 304$). The scale bar is 20 μ m. *, $p < 0.05$.

depends on the local environment. In addition, we demonstrate that the decreased motility of vinculin knockout cells in a three-dimensional environment is attributable to decreased adhesion strength and tractions. These results suggest that vinculin may be an important regulator of metastasis formation and shed light on a molecular mechanism that can influence cell motility as a function of the extracellular environment.

To explain the biochemical and biomechanical function of vinculin in a two-dimensional and a three-dimensional migratory system, we investigated cell adhesiveness (adhesion strength), focal adhesion number and size, cell spreading, cell stiffness and fluidity, cytoskeletal remodeling dynamics, and contractile force generation in MEFvin^{wt/wt} and MEFvin^{-/-} cells. All of these parameters, as well as the matrix degradation through proteolytic enzymes, have been previously shown to influence to a varying degree the cell migration on two-dimensional substrates as well as in a three-dimensional extracellular matrix (2, 4, 26).

The secretion of the matrix metalloproteinase MT1-MMP has been reported to lead to substantial collagen fiber degradation and to be an important marker for the malignancy of several tumors (27, 28). We speculated whether a lower MT1-MMP secretion and consequently lower enzymatic degradation of the ECM may provide an explanation for the decreased invasiveness of MEFvin^{-/-} cells. The cell surface expression of MT1-MMP on MEFvin^{-/-} cells, however, was 8-fold increased, which rules out this mechanism, unless the secreted MT1-MMP protease was functionally impaired. Alternatively, the increased MT1-MMP secretion may have destabilized the collagen-integrin connections (7), which as discussed below, could lead to higher motility in two-dimensional and reduced invasiveness in three-dimensional. To test this possibility, we analyzed the effect of a broadband MMP inhibitor (GM6001) on cell invasion. We found that the addition of GM6001 did not cause changes in cell invasion of MEFvin^{wt/wt} cells and slightly increased cell invasion in MEFvin^{-/-} cells, but the differences in their invasiveness remained nonetheless large. These data demonstrate that MMP secretion played little if any role in vinculin-facilitated cell invasion.

The adhesion strength characterizes the ability of cells to attach tightly to the substrate. On the one hand, a reduction in adhesion strength is thought to decrease invasiveness by preventing the cells from developing sufficient traction, which is needed to overcome the steric hindrance of three-dimensional collagen matrices (26). On the other hand, a reduction in adhesion strength can lead to increased two-dimensional motility by lowering the movement-restraining forces at the rear edge of the cell (29). The strength of cell-matrix adhesions is mainly regulated through integrins whose cytoplasmic tail is linked to the actomyosin cytoskeleton through binding of focal adhesion proteins such as vinculin. In this context, vinculin has been described to act as a mechano-coupling protein (8, 9, 30). Here, we found that the adhesion strength of FN-coated beads is 3-fold lower in MEFvin^{-/-} cells compared with MEFvin^{wt/wt} cells, consistent with the notion that the mechano-coupling function of vinculin is important for firm adhesion to the ECM. Alternatively, the decreased density of focal adhesions in MEFvin^{-/-} cells, as indicated by our

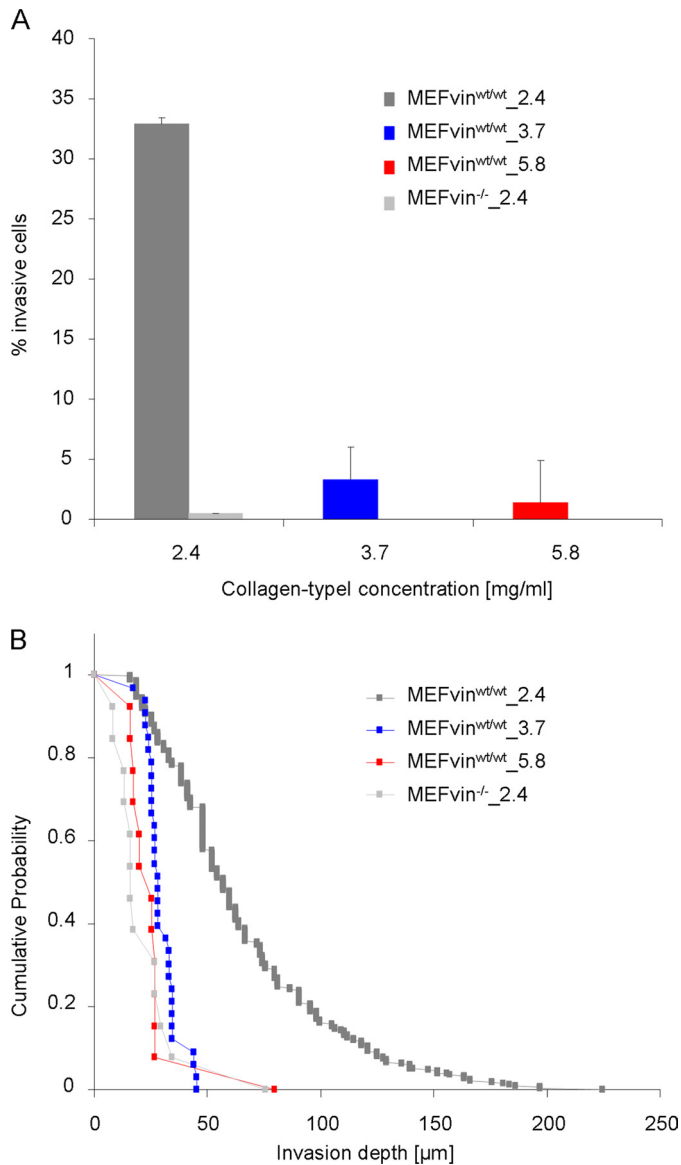


FIGURE 6. Effect of collagen density on the invasion of MEFs. *A*, three different collagen concentrations of 2.4, 3.7, and 5.8 mg/ml were tested for cell invasion. After 3 days, MEFvin^{wt/wt} cells were able to invade all gels, whereas MEFvin^{-/-} cells were able to migrate only into 2.4 mg/ml gels. *B*, invasion profiles of MEFvin^{wt/wt} and MEFvin^{-/-} cells (light gray) in three-dimensional ECMs with different collagen concentrations (red, 5.8; blue, 3.7; dark gray, 2.4).

data, could provide an explanation for their reduced adhesiveness. We ruled out that decreased $\alpha 5\beta 1$ integrin expression levels were responsible for the reduced adhesion strength of MEFvin^{-/-} cells; in fact, our data show that the $\alpha 5\beta 1$ integrin expression was even increased in these cells. Whatever the molecular details are, vinculin-facilitated increased adhesion strength of MEFvin^{wt/wt} cells could lead to increased invasiveness by enhancing the transmission and generation of contractile forces compared with MEFvin^{-/-} cells.

Further, we tested whether the mechano-coupling protein vinculin influences other mechanical properties of cells that are known to affect cell invasiveness into dense three-dimensional ECMs. A previous study of different metastatic cancer cells reported that primary metastatic cancer cells and metastatic cancer cell lines were more deformable compared with non-

metastatic cells, and it can be argued that this is because they can squeeze more easily through the pores of a dense three-dimensional ECM (31). Because the deformability of cells can be decomposed into a stiffness and a fluidity component, we determined both of them separately in this study.

Cell fluidity, which is a measure of the speed of cytoskeletal remodeling processes, was estimated from the power law exponent *b* of the creep response of cytoskeletally bound beads. MEFvin^{-/-} cells were more fluid-like than MEFvin^{wt/wt} cells, which is consistent with their increased migration speed in a two-dimensional environment but not with their decreased three-dimensional motility. Cell stiffness was measured as the inverse of prefactor *a* of the creep response. MEFvin^{-/-} cells were 2-fold softer compared with MEFvin^{wt/wt} cells, which again is consistent with their increased migration speed in a two-dimensional environment but not with their decreased three-dimensional motility.

These results are consistent with a recent study in which we reported that mouse embryonic carcinoma F9 vinculin knockout cells (F9vin^{-/-} cells) were softer and more fluid-like compared with F9 wild-type (F9vin^{wt/wt}) cells (9). Moreover, in that study we reported that F9vin^{wt/wt} cells were considerably more contractile than F9vin^{-/-} cells (9). When we decreased the contractility of MEFs by inhibition of myosin light chain kinase activity using ML-7, cell stiffness of both MEFs collapsed to nearly identical levels. This result indicates that MEFvin^{wt/wt} cells had a higher contractility before ML-7 addition, because cell stiffness and contractility are closely linked in well spread adherent cells (25). Traction force measurements directly confirmed that the stiffer MEFvin^{wt/wt} cells generate 3-fold higher contractile forces compared with MEFvin^{-/-} cells. Notably, the magnitude of contractile forces of MEFvin^{wt/wt} cells is comparable with those of highly invasive human MDA-MB-231 breast carcinoma cells (13).

Although the biochemical signaling pathway responsible for the higher contractility in vinculin-expressing cells remains elusive (9), the mechanical “pathway” seems straightforward: higher forces in vinculin-expressing cells help to overcome the steric constraints of dense three-dimensional ECMs. To test this hypothesis, we analyzed the effect of stiffer and denser ECMs on cell invasion. As expected, an increase in steric hindrance only reduced the invasiveness of the stronger MEFvin^{wt/wt} cells but completely abolished the invasiveness of the weaker MEFvin^{-/-} cells.

In summary, we found that vinculin exhibits a dual function in cell migration, depending on the environment. The stabilization of focal adhesions and cytoskeletal structures by vinculin impedes two-dimensional migration. At the same time, vinculin facilitates contractile force generation, which enhances cell invasion by helping the cell to overcome the steric hindrance of dense three-dimensional ECMs.

Acknowledgments—We thank Dr. Eileen Adamson for the kind gift of the MEF cells; Dr. Klemens Rottner for the help with the generation of large T immortalized MEF cells; Dr. Jürgen Behrens, Dr. Jan Brabek, and Dr. Staffan Johansson for critical reading of the manuscript and helpful discussions; Barbara Reischl and Christine Albert for excellent technical assistance; and Ulrike Scholz for help with the manuscript.

Vinculin Facilitates Cell Invasion

REFERENCES

- Horwitz, A. R., and Parsons, J. T. (1999) *Science* **286**, 1102–1103
- Mierke, C. T., Rösel, D., Fabry, B., and Brábek, J. (2008) *Eur. J. Cell Biol.* **87**, 669–676
- Lauffenburger, D. A., and Horwitz, A. F. (1996) *Cell* **84**, 359–369
- Friedl, P., and Bröcker, E. B. (2000) *Cell Mol. Life Sci.* **57**, 41–64
- Webb, D. J., Brown, C. M., and Horwitz, A. F. (2003) *Curr. Opin. Cell Biol.* **15**, 614–620
- Friedl, P., and Wolf, K. (2003) *Nat. Rev. Cancer* **3**, 362–374
- Wolf, K., Mazo, I., Leung, H., Engelke, K., von Andrian, U. H., Deryugina, E. I., Strongin, A. Y., Bröcker, E. B., and Friedl, P. (2003) *J. Cell Biol.* **160**, 267–277
- Ezzell, R. M., Goldmann, W. H., Wang, N., Parasharama, N., and Ingber, D. E. (1997) *Exp. Cell Res.* **231**, 14–26
- Mierke, C. T., Kollmannsberger, P., Zitterbart, D. P., Smith, J., Fabry, B., and Goldmann, W. H. (2008) *Biophys. J.* **94**, 661–670
- Goldmann, W. H., Schindl, M., Cardozo, T. J., and Ezzell, R. M. (1995) *Exp. Cell Res.* **221**, 311–319
- Subauste, M. C., Pertz, O., Adamson, E. D., Turner, C. E., Junger, S., and Hahn, K. M. (2004) *J. Cell Biol.* **165**, 371–381
- Saunders, R. M., Holt, M. R., Jennings, L., Sutton, D. H., Barsukov, I. L., Bobkov, A., Liddington, R. C., Adamson, E. A., Dunn, G. A., and Critchley, D. R. (2006) *Eur. J. Cell Biol.* **85**, 487–500
- Mierke, C. T., Zitterbart, D. P., Kollmannsberger, P., Raupach, C., Schlötzer-Schrehardt, U., Goecke, T. W., Behrens, J., and Fabry, B. (2008) *Biophys. J.* **94**, 2832–2846
- McNulty, A. L., Weinberg, J. B., and Guilak, F. (2009) *Clin. Orthop. Relat. Res.* **467**, 1557–1567
- Kollmannsberger, P., and Fabry, B. (2007) *Rev. Sci. Instrum.* **78**, 114301–114306
- Fabry, B., Maksym, G. N., Butler, J. P., Glogauer, M., Navajas, D., and Fredberg, J. J. (2001) *Phys. Rev. Lett.* **87**, 148102–148106
- Pelham, R. J., Jr., and Wang, Y. (1997) *Proc. Natl. Acad. Sci. U.S.A.* **94**, 13661–13665
- Raupach, C., Zitterbart, D. P., Mierke, C. T., Metzner, C., Müller, F. A., and Fabry, B. (2007) *Phys. Rev. E Stat. Nonlin Soft Matter. Phys.* **76**, 011918
- Butler, J. P., Toliā-Nçrrelykke, I. M., Fabry, B., and Fredberg, J. J. (2002) *Am. J. Physiol. Cell Physiol.* **282**, C595–C605
- Coll, J. L., Ben-Ze'ev, A., Ezzell, R. M., Rodríguez Fernández, J. L., Baribault, H., Oshima, R. G., and Adamson, E. D. (1995) *Proc. Natl. Acad. Sci. U.S.A.* **92**, 9161–9165
- Xu, W., Coll, J. L., and Adamson, E. D. (1998) *J. Cell Sci.* **111**, 1535–1544
- Dieterich, P., Klages, R., Preuss, R., and Schwab, A. (2008) *Proc. Natl. Acad. Sci. U.S.A.* **105**, 459–463
- Baciu, P. C., Suleiman, E. A., Deryugina, E. I., and Strongin, A. Y. (2003) *Exp. Cell Res.* **291**, 167–175
- Fabry, B., and Fredberg, J. J. (2003) *Respir. Physiol. Neurobiol.* **137**, 109–124
- Wang, N., Toliā-Nçrrelykke, I. M., Chen, J., Mijailovich, S. M., Butler, J. P., Fredberg, J. J., and Stamenoviā, D. (2002) *Am. J. Physiol. Cell Physiol.* **282**, C606–C616
- Zaman, M. H., Trapani, L. M., Siemeski, A., Mackellar, D., Gong, H., Kamm, R. D., Wells, A., Lauffenburger, D. A., and Matsudaira, P. (2006) *Proc. Natl. Acad. Sci. U.S.A.* **103**, 10889–10894
- Okada, A., Bellocq, J. P., Rouyer, N., Chenard, M. P., Rio, M. C., Chambon, P., and Basset, P. (1995) *Proc. Natl. Acad. Sci. U.S.A.* **92**, 2730–2734
- Davidson, B., Goldberg, I., Gotlieb, W. H., Kopolovic, J., Ben-Baruch, G., Nesland, J. M., Berner, A., Bryne, M., and Reich, R. (1999) *Clin. Exp. Metastasis* **17**, 799–808
- Gallant, N. D., Michael, K. E., and García, A. J. (2005) *Mol. Biol. Cell* **16**, 4329–4340
- Möhl, C., Kirchgessner, N., Schäfer, C., Küpper, K., Born, S., Diez, G., Goldmann, W. H., Merkel, R., and Hoffmann, B. (2009) *Cell Motil. Cytoskeleton* **66**, 350–364
- Guck, J., Schinkinger, S., Lincoln, B., Wottawah, F., Ebert, S., Romeyke, M., Lenz, D., Erickson, H. M., Ananthakrishnan, R., Mitchell, D., Käs, J., Ulvick, S., and Bilby, C. (2005) *Biophys. J.* **88**, 3689–3698